Global Change Biology (2005) **11,** 2177–2195, doi: 10.1111/j.1365-2486.2005.01068.x

Climatic and ecological determinants of leaf lifespan in polar forests of the high CO_2 Cretaceous 'greenhouse' world

S. J. BRENTNALL*, D. J. BEERLING*, C. P. OSBORNE*, M. HARLAND†, J. E. FRANCIS†, P. J. VALDES‡ and V. E. WITTIG§

Department of Animal and Plant Sciences, University of Sheffield, Sheffield S10 2TN, UK, †School of Earth and Environment, University of Leeds, Leeds LS2 9JT, UK, ‡School of Geographical Sciences, University of Bristol, Bristol BS8 1SS, UK, §Department of Plant Biology, University of Illinois at Urbana-Champaign, IL 61801-3838, USA

Abstract

Polar forests once extended across the high-latitude landmasses during ice-free 'greenhouse' intervals in Earth history. In the Cretaceous 'greenhouse' world, Arctic conifer forests were considered predominantly deciduous, while those on Antarctica contained a significantly greater proportion of evergreens. To investigate the causes of this distinctive biogeographical pattern, we developed a coupled model of conifer growth, soil biogeochemistry and forest dynamics. Our approach emphasized general relationships between leaf lifespan (LL) and function, and incorporated the feedback of LL on soil nutrient status. The model was forced with a mid-Cretaceous 'greenhouse' climate simulated by the Hadley Centre GCM. Simulated polar forests contained mixtures of dominant LLs, which reproduced observed biogeographical patterns of deciduous, mixed and evergreen biomes. It emerged that disturbance by fire was a critical factor. Frequent fires in simulated Arctic ecosystems promoted the dominance of trees with short LLs that were characterized by the rapid growth and colonization rates typical of today's boreal pioneer species. In Antarctica, however, infrequent fires allowed trees with longer LLs to dominate because they attained greater height, despite slower growth rates. A direct test of the approach was successfully achieved by comparing modelled LLs with quantitative estimates using Cretaceous fossil woods from Svalbard in the European Arctic and Alexander Island, Antarctica. Observations and the model both revealed mixed Arctic and evergreen Antarctic communities with peak dominance of trees with the same LLs. Our study represents a significant departure from the long-held belief that leaf habit was an adaptation to warm, dark winter climates, and highlights a previously unrecognized role for disturbance (in whatever guise) in polar forest ecology.

Keywords: biogeochemistry, disturbance, fossils, leaf lifespan, modelling, polar forests

Received 18 February 2005; and accepted 1 August 2005

Introduction

Fossil evidence indicating that forests once extended to latitudes of 85°N and S provides a tangible reminder of a unique, but now extinct, biome existing for at least the last 350 million years of Earth history (Spicer & Chapman, 1990). In stark contrast with today's high-latitude forests, this biome flourished in a warm 'greenhouse' climate with high atmospheric CO_2 levels (Crowley & Berner, 2001), mild, possibly frost-free winter temperatures (Tarduno *et al*., 1998; Tripati *et al*., 2001; Dutton *et al*., 2002) and, at a latitude of 85°, experienced 5 months of darkness during the polar winter and an equal period of continuous sunlight during the summer. Since the late 1940s, the predominant world view of polar forests has been that their deciduous character represented an adaptation to winter darkness, allowing the trees to avoid the high respiratory losses associated with maintaining a canopy of leaves during the warm winter (Chaney, 1947; Axelrod, 1966; Hickey, 1984; Wolfe, 1985). However, this carbon balance view was

Correspondence: David Beerling,
e-mail: d.j.beerling@sheffield.ac.uk

not universally accepted, even at the time it was first proposed (Mason, 1947; Creber & Chaloner, 1985; Read & Francis, 1992), and results from recent experiments and numerical modelling studies (Beerling & Osborne, 2002; Osborne & Beerling, 2003; Royer *et al*., 2003, 2005) have failed to provide supporting evidence. Indeed, under experimental conditions, the quantity of carbon lost annually by deciduous trees through leaf shedding exceeded that lost by evergreen trees through winter respiration and more limited leaf loss (Royer *et al*., 2003, 2005). Even at the scale of whole forest ecosystems, the deciduous leaf habit was approximately twice as expensive in terms of winter carbon loss as its evergreen counterpart.

Our understanding of the significance of leaf habit for polar forest ecology therefore requires rethinking (Osborne *et al*., 2004). We suggest attention might usefully shift from the simple evergreen vs. deciduous dichotomy towards one considering leaf lifespan (LL, average leaf retention time) along a continuous spectrum running from a quick to slow return on investments of nutrient and dry mass (Kikuzawa, 1991; Reich *et al*., 1997; Givnish, 2002; Grubb, 2002; Wright *et al*., 2004). Global surveys reveal that key leaf traits dictating resource investment and return vary with LL in a manner that alters vegetation function (e.g. evapotranspiration, net primary productivity (NPP)), structure, and nutrient cycling (e.g. albedo, tree height) (Reich *et al*., 1997, 1999; Wright *et al*., 2004). These emerging views of leaf investment strategies are particularly timely in the context of polar forests because new techniques in palaeobotany now allow estimation of LL for extinct species by analysing cellular patterns in the growth rings of fossil wood (Falcon-Lang, 2000a, b). LL, therefore, provides a promising means of realistically uniting past and present forest ecology, and investigating the underlying reasons for the composition of long-extinct high-latitude forests, whose dynamics cannot be inferred directly from fossil remains.

Here, we present a numerical modelling investigation developing this new line of ecological enquiry for the conifer-dominated polar forests of the Cretaceous. We analyse the effect of LL on the functioning of polar forests, with the aim of determining its significance for forest composition, a product evaluated against the fossil record. Critically, we interrogate model simulations to uncover the key mechanisms responsible for distinctive patterns of polar forest biogeography now beginning to emerge from the fossil record (Spicer & Parrish, 1986; Falcon-Lang & Cantrill, 2000, 2001a, b). These indicate that, rather than being of a uniformly deciduous character, high-latitude forests of the Cretaceous were deciduous in the Arctic region, but predominantly evergreen in Antarctica.

Our approach utilizes the University of Sheffield Conifer Model (USCM), a process-based forest growth model that scales-up from generalized relationships between LL, leaf traits and climate (Osborne & Beerling, 2002a). The USCM has been extended and modified by coupling it with a soil biogeochemistry module (Parton *et al*., 1993) to incorporate self-consistent nutrient limitations by simulating belowground carbon and nitrogen cycling. Simulated structural and functional characteristics of trees drive a forest dynamics scheme in which height is determined from hydraulic constraints, wood production and time since last disturbance (Whitehead *et al*., 1984; Margolis *et al*., 1995; Osborne & Beerling, 2002b), and Lotka–Volterra equations for representing interspecific competition (Silvertown & Lovett-Doust, 1993; Cox, 2001).

We focus on the mid-Cretaceous (Aptian, 124–112 Ma) because it represents a time of global warmth (Spicer & Corfield, 1992) and the heyday of polar forests (Spicer & Parrish, 1986). We developed both qualitative and quantitative palaeodatasets to evaluate simulations of polar forest distribution and composition against observations. The qualitative dataset was compiled by analysing information from published sources describing the presumed leaf habit (evergreen vs. deciduous) of fossil plant assemblages and has the more extensive geographical coverage. While it only gives an indication of the predominant leaf habit for forests at a particular locality, it highlights regional-scale biome distributions and serves as a valuable guide for evaluating model performance. The quantitative dataset provides estimates of LL for comparison with USCM predictions and derives from analysis of Cretaceous fossil woods from Svalbard in the high northern latitudes (this paper) and Alexander Island, Antarctica (Falcon-Lang & Cantrill, 2000, 2001a, b; Falcon-Lang, 2000a, b).

Materials and methods

Coupled USCM description

The forest growth module of the coupled USCM, described and validated in detail elsewhere (Osborne & Beerling, 2002a), considers four biogeochemical and biophysical aspects of forest function in relation to LL: (i) carbon exchange between vegetation and the atmosphere; (ii) fluxes of water through the soil–plant–atmosphere continuum; (iii) limitation of tree growth by nitrogen; and (iv) land surface-atmosphere energy exchange. In the model, LL directly influences the nitrogen content of tissues and leaf mass: area ratios (Reich *et al*., 1998; 1999), which then determine leaf capacities for photosynthesis, respiration and stomatal conductance. Photosynthetic carbon uptake is described by the

Farquhar *et al*. (1980) biochemical model and scaled to the canopy using a 'sun-shade' approach (DePury & Farquhar, 1997). This canopy scheme accounts for distributions of nitrogen and photosynthetic enzymes within the canopy, and sunlit and shaded fractions of leaves. Plant respiration is dependent upon temperature and tissue nitrogen contents (Ryan *et al*., 1996). Evapotranspiration follows the Penman–Monteith method (Penman, 1948; Monteith, 1965), accounting for stomatal responses to soil water, atmospheric humidity and CO_2 (Leuning, 1995), the dependence of aerodynamic roughness on canopy leaf area (Shaw & Pereira, 1982), and the limitation of soil evaporation by surface moisture content (Chanzy & Bruckler, 1993). Nitrogen uptake depends on the mass of roots, temperature and soil nitrogen content (Woodward *et al*., 1995). A further limitation is imposed by the soil carbon content, which influences mycorrhizal associations of trees and their ability to extract organic nitrogen (Woodward & Smith, 1994). Energy exchange between vegetation, soil and the atmosphere accounts for short-wave, long-wave (upward and downward), latent and sensible heat fluxes. The absorption of solar energy in both the visible and near-infrared wavebands is considered for the leaf canopy and soil (Weiss & Norman, 1985; DePury & Farquhar, 1997). Forest energy budget, evapotranspiration and photosynthesis are interdependent, and solved numerically. The leaf area index (LAI), a key determinant of energy, water and carbon fluxes in the model, is calculated after accounting for the limitations on growth imposed by water, nitrogen and light (Osborne & Beerling, 2002a).

The soil module newly incorporated for this paper is based upon the Century model of carbon and nitrogen dynamics (Parton *et al*., 1993) (Fig. 1). Eight soil carbon and nitrogen pools are modelled, each distinguished by their different maximum decomposition rates: two surface litter pools, representing the more recalcitrant (e.g. lignin, cellulose) and more labile (e.g. sugars) components, respectively, two similar pools for subsurface (especially root) litter; surface and soil microbial (active) pools; and pools of slow and passive soil organic matter (Fig. 1). Decomposition rates, and fluxes of carbon between the pools, are calculated as functions of soil moisture and temperature. Nitrogen fluxes and the C : N ratio of each reservoir are controlled by the size of a further pool, mineral nitrogen, which is in turn affected by the implied net mineralization or immobilization of the other pools. Each nitrogen flux is equal to the product of the corresponding carbon flux and the N : C ratio of the pool receiving the flow. Soil carbon and nitrogen dynamics are described by nonlinear differential equations with parameters depending on soil texture, temperature, precipitation, humidity, soil moisture, water flow, potential evaporation, litter quantity and quality. The equations are solved on a monthly time step.

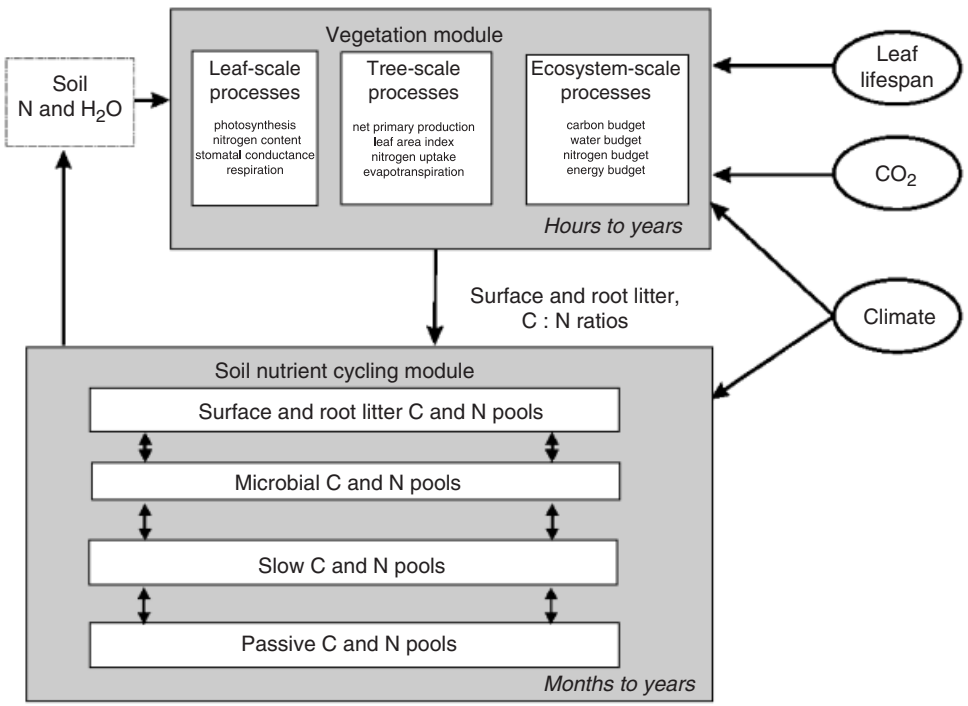

Fig. 1 Schematic diagram of key forest processes from the leaf to the regional scale simulated in the above- and below-ground modules of the University of Sheffield Conifer Model.

The model requires inputs of monthly temperature, relative humidity and precipitation, which for the Cretaceous simulations were derived from the Hadley Centre general circulation model (GCM). Successful validation of the USCM under the present-day climate and atmospheric CO_2 concentration was achieved on a site-by-site basis by comparing predictions and observations of LAI and NPP from conifer forest across a wide climatic gradient and, at the regional scale, by comparison with satellite products (see Appendix A).

Forest dynamics scheme

The coupled USCM simulates the properties of a monoculture forest of a given LL growing within each grid-box. We performed parallel simulations for trees with a range of LLs, to determine the composition of the forest using a form of Lotka–Volterra dynamics. In this scheme, the exponential rate of colonization by trees of each LL is limited by both intra- and interspecific competition. Competition is proportional to the product of the two population sizes in question (Silvertown & Lovett-Doust, 1993). Inclusion of intraspecific competition means that the growth term can alternatively be seen as logistic. The version we use also includes a term representing exogenous mortality because of fire, giving (Cox, 2001):

$$C_i \frac{\mathrm{d}v_i}{\mathrm{d}t} = \lambda_i \Pi_i v_i \left\{ 1 - \sum_{j=1}^{n} c_{ij} v_j \right\} - \gamma_v v_i C_i, \qquad (1)$$

where $i = 1, 2, \ldots, n$ is an index for each of the functional types (FTs) considered. C_i is biomass C per unit land surface area for the FT with the ith LL, and v_i the fraction of the grid-box covered by trees of this type. λ_i is a partitioning coefficient representing the fraction of NPP used for increasing tree numbers, rather than the size of individual trees (i.e. λ is a measure of the reproductive effort). Π_i is the aboveground NPP per unit vegetated area ($\mathrm{g\,C\,m^{-2}\,yr^{-1}}$), c_{ij} is a competition coefficient in the range [0, 1] representing the effect *on* FT *i of* type *j*, and γ_v is a large-scale disturbance rate. Disturbance by fire is computed with a fire module, based on temperature and precipitation, and which has been validated against satellite wildfire datasets (Beerling & Woodward, 2001; Woodward *et al*., 2001).

Early successional woody plant species generally have faster rates of photosynthesis and respiration, higher stomatal conductance, and more efficient nutrient uptake mechanisms, than their late successional counterparts (Bazzaz, 1979, 1996; Grime, 2001), all traits strongly associated with shorter LLs (Reich *et al*., 1999; Wright *et al*., 2004). Consistent with this observation, trees of relatively short LL, for instance larches, birches, aspen or white pine, commonly act as pioneer species after disturbance in today's boreal or Alpine forests (Didier, 2001; Schulze *et al*., 2002; Doležal *et al*., 2004; Jain *et al*., 2004). Although some of these pioneer species are deciduous angiosperms, we assume that functionally similar gymnosperms fulfilled this role in the Early to mid-Cretaceous, when angiosperms had not yet evolved to the point of becoming dominant trees (Crane, 1987; Hill & Scriven, 1995). To reflect the tendency for trees of shorter LL to be more effective colonizers, we define the partitioning coefficient λ (for each i) to be a decreasing function of LL, and an increasing function of LAI, as follows. Denoting LL (in months) by L, we set λ to zero, so that all the production is channelled towards increasing the size of individual trees, if the LAI is less than

$$L_{\min} = \begin{cases} 0 & \text{if } L < 4, \\ (L-4)/24 & \text{if } 4 \le L \le 28, \\ 1 & \text{if } 28 < L. \end{cases} \qquad (2)$$

If the LAI is greater than

$$L_{\max} = \begin{cases} (L+44)/12 & \text{if } L \le 68, \\ 9 & \text{otherwise}, \end{cases} \qquad (3)$$

then λ is set to 1, so that essentially all the production of mature trees goes towards reproduction. λ varies linearly between these two values of LAI, for a given value of LL. Thus, the shorter the LL, the lower the LAI at which some of the production is diverted towards colonization; and the larger the LAI (for a given LL), the larger the fraction of production going towards colonization.

We define the competition coefficients as follows (Cox, 2001):

$$c_{ij} = \begin{cases} 1, & i = j, \\ 1/[1 + \exp\{20(h_i - h_j)/(h_i + h_j)\}], & i \ne j, \end{cases} \qquad (4)$$

where h_i is the height attained by trees of type i in one fire return interval. This represents competition for light. If $h_j \gg h_i$, the coefficient is close to 1; tree type j, being much taller than type i, exerts a large negative influence on the latter through shading. Conversely, if $h_j \ll h_i$ the coefficient approaches zero.

At equilibrium, $\mathrm{d}v_i/\mathrm{d}t = 0$, and (1) becomes a system of n linear simultaneous equations in the vegetated fractions v_i, provided that these are all nonzero. In matrix notation, this system is

$$\mathbf{Cv} = \mathbf{a}, \qquad (5)$$

where $\mathbf{C}$ is the $n \times n$ matrix of competition coefficients c_{ij}, $\mathbf{v}$ the vector of vegetated fractions, and $\mathbf{a}$ is a vector with elements

$$a_i = 1 - \frac{\gamma_v C_i}{\lambda_i \Pi_i}. \qquad (6)$$

Note that a_i is the vegetated fraction that would be obtained if $\mathbf{C}$ were the unit matrix (i.e. represents the

potential vegetated fraction achieved in the absence of competition from other tree types). It is less than 1 because only a finite time, $1/\gamma_v$, is available for recolonization between disturbances, the colonization rate, proportional to $\lambda\Pi/C$, is also finite, and the colonization process is effectively logistic (i.e. self-limiting). The faster the colonization rate, compared with the disturbance frequency, the closer the potential vegetated fraction is to 1. Conversely, if $\gamma_v C_i/\lambda_i\Pi_i > 1$ (i.e. the disturbance exceeds the colonization rate) we set $a_i = 0$; this represents, for example, the case where trees do not grow vigorously enough to set seed, and subsumes the case where LAI $< L_{\min}$ (i.e. $\lambda = 0$). Note that C_i/Π_i has units of time, and represents the turnover time taken for the biomass to be replenished by new production in the dynamic equilibrium between production and decomposition. Therefore, Π_i/C_i is a stand-level growth rate, and $\lambda_i\Pi_i/C_i$ a measure of the rate at which disturbed land is recolonized by trees of type i, in the absence of competition.

We solved Eqn (5) at each grid point by inverting **C**, after excluding LLs unable to grow (or reproduce) at that site because of the climate. The final vegetated fractions are given by

$$\mathbf{v} = \mathbf{C}^{-1}\mathbf{a}. \tag{7}$$

This sometimes yields negative v_i values, indicating that type i is outcompeted to extinction; in this case v_i is set to zero.

The (potential) aboveground biomass $C_i^{\text{pot}}(\text{g C m}^{-2})$ accumulating if the trees were allowed to grow to their full height $h_i^{\max}$(m), undisturbed by fire or competition, is calculated as the product of the mass of a single trunk and the number of trees per unit area (Enquist *et al*., 1998). Representing a tree trunk as a cylinder of radius $h_i^{\max}/100$, height $h_i^{\max}$ and density 392 kg m^{-2}, of which 40% is carbon (Osborne & Beerling, 2002b), the potential aboveground biomass is given by

$$C_i^{\text{pot}} = 1251(h_i^{\max})^{3/4}. \tag{8}$$

The USCM calculates $h_i^{\max}$ using the hydraulic model of Whitehead *et al*. (1984), in which height is inversely proportional to the square root of an evaporative demand (Koch *et al*., 2004). Since stomatal conductance and therefore evaporative demand decrease with increasing LL, trees with longer-lived leaves tend to be taller, other things being equal (see Osborne & Beerling, 2002b).

Assuming that biomass carbon accumulates annually according to the NPP until this maximum or equilibrium value is reached, or until disturbance occurs (whichever happens first), the final tree height is given by

$$h_i = \min\left(h_i^{\max}, \frac{\Pi_i(h_i^{\max})^{1/4}}{1251\gamma_v}\right) \tag{9}$$

and the required biomass C_i is obtained by using this value for the height in the right-hand side of Eqn (8). The structure of our FT model is illustrated in Fig. 2.

To obtain polar biome maps suitable for comparison with our qualitative palaeodataset, and for validation against modern data, vegetated fractions v_i with different LLs were aggregated to give 'deciduous' f_d (LL $<$12 months) and 'evergreen' fractions f_e (LL $\geq$ 12 months). The results of this procedure were not sensitive to the number of different deciduous and evergreen LLs used. Dominant LLs were defined according to v_i. Biome distribution was optimized through Eqns (2) and (3),

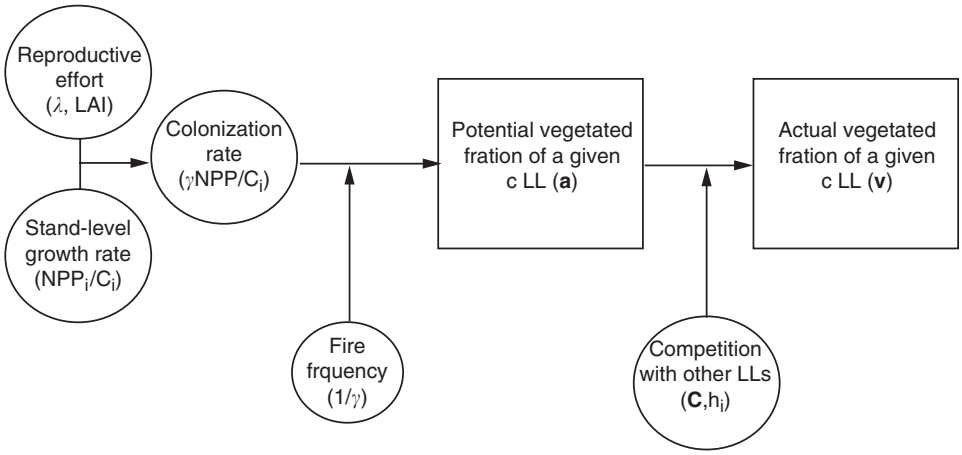

Fig. 2 Diagrammatic representation of the forest dynamic scheme implemented with the University of Sheffield Conifer Model. Stand-level growth is partitioned between either reproduction or colonization and over a specific time that depends on disturbance by fire, and leads to the potential cover of a given pixel. The actual vegetation cover determined by competition with other trees with leaves of different leaf lifespans.

and f_d and f_e, to reproduce the extent of northern boreal forest biomes (evergreen and deciduous needle-leaved trees) categorized by the International Satellite Land Surface Climatology Project (ISLSCP) (Meeson *et al*., 1995). The κ statistic is a measure, albeit imperfect (Beerling & Woodward, 2001), of how well categorical dataset reproduces another, and was highly significant ($\kappa = 24.3\%$, $P < 0.001$).

Mid-Cretaceous global climate simulation

We forced the coupled USCM with a mid-Cretaceous (Aptian) climate simulation produced by the latest generation of the Hadley Centre Atmospheric GCM (HadAM3) (Pope *et al*., 2000). HadAM3 is based on the UK Meteorological Office GCM (Hewitt & Mitchell, 1996) and operates with a spatial resolution of 3.75° longitude × 2.5° latitude and 19 vertical levels. Prescribed zonally symmetric sea-surface temperatures (SSTs) of 30cos(lat) °C were used; implying an increased poleward transport of the ocean heat flux compared with the present day situation. The simulation employed the reconstructions of mid-Cretaceous coastlines and the positions of major mountain ranges described by Smith *et al*. (1994). Atmospheric CO_2 levels were set at 1300 ppm as the mean of the various proxy estimates (Crowley & Berner, 2001; Royer *et al*., 2004). The integration was run for 14 model years and the Aptian 'climate' taken as the average of the last 10 years.

Numerical model experiments

The USCM was run separately for trees with nine different LLs (4, 6, 9, 12, 18, 24, 48, 72 and 96 months), using both a modern climatology for the years 1982–1991, derived from the UEA dataset (New *et al*., 1999, 2000), and an Aptian climatology as modelled by HadAM3. Both climatologies were global in extent, at a resolution of 3.75° in both latitude and longitude.

Polar forest reconstructions

A qualitative dataset of polar and temperate forest biome distributions in the Early and Late Cretaceous was compiled from published literature sources (Table 1). Biomes were classified as deciduous, mixed or evergreen using evidence from macrofossil floras (leaf and wood), palynological records or the analysis of dispersed leaf cuticles. We followed the published interpretations of fossil records in assigning biome types which used a range of methods to obtain evidence about leaf habit: wood anatomy (Falcon-Lang, 2000a, b); analysis of leaf traces (Falcon-Lang & Cantrill, 2001a); examination of leaf physiognomy and cuticle morphology (Chaloner & Creber, 1990); comparison with nearest living relatives (NLRs) (Chaloner & Creber, 1990); and interpretation of taphonomy (preservational setting) (Spicer & Parrish, 1986). While none of these methods is without its difficulties, we have accepted at face value the authors' original interpretation, but attempted to draw upon more than one line of evidence when possible for any particular site.

Wood anatomy provides a proxy record of leaf habit that is proving useful in palaeoecological reconstructions (Falcon-Lang & Cantrill, 2000, 2001a, b). It is based on the general observation that trees with short-lived leaves produced pronounced annual growth rings, whereas those with long-lived foliage form less distinct ring boundaries (Falcon-Lang, 2000a, b). Leaf traces connect the vascular system of leaves with the xylem of branch wood in tree species, are extended by secondary growth every year that the leaf persists, and remain in wood after leaf abscission. Palaeobotanists may therefore obtain a very precise measure of LL from fossil woods by counting the number of annual growth rings bisected by the xylem strand of leaf traces, although these are infrequently preserved (Falcon-Lang & Cantrill, 2001a, b). Physiognomy describes the form and structure of fossils, and may be used to provide clues about the habit of leaves, via characters such as leaf or cuticle thickness and sunken stomata (Chaloner & Creber, 1990), although these are necessarily speculative. The NLR method assumes that closely related fossil and modern plant taxa share common traits such as LL, but is difficult to apply for the Cretaceous, where the phylogenetic distance between ancient and modern species is significant (Chaloner & Creber, 1990). Taphonomy is the study of the depositional and fossilization process, and may provide important inferences about leaf habit, especially through the interpretation of leaf mats as characteristic of deciduous species, with leaves spread randomly throughout a sequence characterizing evergreens (Spicer & Parrish, 1986).

We obtained new quantitative datasets for LL by analysing Cretaceous fossil conifer woods using the approach of Falcon-Lang (2000a, b). The technique follows from the observation that the markedness of boundaries between annual growth rings in modern trees from seasonal climates is correlated with LL (Falcon-Lang, 2000a, b). To obtain LLs for fossil woods, we, therefore, used a newly developed modern calibration dataset for contemporary conifers consisting of 21 modern tree species, with nineteen from the Northern Hemisphere and two from the Southern Hemisphere (Harland, 2005). For each genus, the ring markedness index (RMI) was calculated as $RMI = PD \times PL/100$, where PD is the percentage diminution and PL the percentage latewood (Falcon-Lang, 2000a, b). The PD

Table 1 Leaf habit of Cretaceous polar forests inferred from a qualitative interpretation of plant fossils

Fossil locality	Fossil type	Age	Palaeo-lat	Palaeo-lon	Leaf habit	Methods	References
North America (Arctic)							
Alaska, Nanushuk group	L, W	EC	78°N	52°W	D	LP, NLR, T	Spicer & Parrish (1986)
West Greenland	L	LC	65°N	10°E	M	NLR	Boyd (1994)
West Greenland	L, W	LC	68°N	10°E	M	NLR	Seward (1926)
Montana, Kootenai formation	L	EC	50°N	40°W	M	LP	Upchurch & Wolfe (1993)
Canada, western interior	L, W	EC	60°N	50°W	M	LP, T	Upchurch & Wolfe (1993)
Alaska, Kuk river basin	L	EC	85°N	60°W	M	NLR	Smiley (1976); Axelrod (1984)
Alaska, Nanushuk group	L, W	LC	78°N	52°W	D	LP, NLR, T	Spicer & Parrish (1986)
Canada, Mackenzie Delta	P	LC	74°N	38°W	M	LP, NLR,	Upchurch *et al*. (1999)
West Greenland	L	LC	56°N	5°E	E	LP, T	Upchurch *et al*. (1999)
Alaska, North Slope	L	LC	81°N	45°W	D	LP, T	Upchurch *et al*. (1999)
Alaska, North Slope	P	LC	85°N	35°W	D	LP, T	Upchurch *et al*. (1999)
Canada, Bathurst Island	P	LC	74°N	8°W	D	LP, T	Upchurch *et al*. (1999)
Eurasia (Arctic)							
Svalbard, Spitzbergen	W	EC	68°N	50°E	M	WA	Harland & Francis (this paper)
Russia, western Siberia	L	LC	70°N	85°E	D	LP	Herman (1994)
Russia, Severnaya Zemlya	L	LC	80°N	120°E	D	LP	Herman (1994)
Russia, central Siberia	L	LC	68°N	125°E	D	LP	Herman (1994)
Russia, Dzhagdy Mountains	L	LC	65°N	150°E	D	LP	Herman (1994)
Russia, Vladivostok region	L	LC	60°N	145°E	D	LP	Herman (1994)
Russia, Okhotsk region	L	LC	70°N	150°E	D	LP	Herman (1994)
Russia, Okhotsk region	L	LC	70°N	155°E	D	LP	Herman (1994)
Russia, Kamchatka	L	LC	72°N	170°E	D	LP	Herman (1994)
W. Siberia, Vakh River	P	LC	55°N	75°E	D	LP, T	Upchurch *et al*. (1999)
E. Siberia, Koryak Range	L	LC	80°N	125°W	D	LP, T	Upchurch *et al*. (1999)
E. Siberia, Beloye Mt.	L	LC	70°N	150°E	D	LP, T	Upchurch *et al*. (1999)
W. Siberia, Berezovo	P	LC	50°N	65°E	D	LP, T	Upchurch *et al*. (1999)
C. Siberia, Vilyuv	L	LC	70°N	90°E	D	LP, T	Upchurch *et al*. (1999)
E. Siberia, Anadyr	L	LC	85°N	125°W	D	LP, T	Upchurch *et al*. (1999)
C. Siberia, Lintsya River	L	LC	73°N	105°E	D	LP, T	Upchurch *et al*. (1999)
E. Siberia, Umkuveyen	L	LC	85°N	120°W	D	LP, T	Upchurch *et al*. (1999)
E. Siberia, Vestrechnoy	L	LC	70°N	120°E	D	LP, T	Upchurch *et al*. (1999)
Gondwanaland (Antarctic)							
Tierra del Fuego	P	EC	48°S	25°W	E	NLR	Dettmann (1989) and Dettman *et al*. (1992)
New Zealand, Middle Clarence Valley	L	EC	68°S	170°E	M	LP, NLR, T	Parrish *et al*. (1998)
Antarctica, Alexander Island	L, W	EC	60°S	57°W	E	WA, LT, LP, NLR, T	Falcon-Lang & Cantrill (2001a)
Australia, Otway & Gippsland Basins	L, W, P	EC	69°S	119°E	M	WA, LP, T	Douglas & Williams (1982)
Antarctica, Livingston Island	L, W, P	EC	54°S	52°W	E	LT, LP, NLR, T	Falcon-Lang & Cantrill (2001b)
Antarctica, Seymour Island	C	LC	56°S	46°W	E	LP, Cm, T	Upchurch & Askin (1989)
New Zealand, Kaitangata Coalfield	C	LC	82°S	155°E	M	LP	Pole & Douglas (1999)
Antarctica, King George Island	L	LC	52.5°S	52°W	E	LP, T	Upchurch *et al*. (1999)

(*continued*)

Table 1 (Contd.)

Fossil locality	Fossil type	Age	Palaeo-lat	Palaeo-lon	Leaf habit	Methods	References
Antarctica, Ross Ice Shelf	P	LC	82°S	170°E	E	LP, T	Upchurch *et al*. (1999)
Antarctica, Weddell Sea	P	LC	64.5°S	17°W	E	LP, T	Upchurch *et al*. (1999)
Antarctica, West Ice Shelf	P	LC	62.5°S	110°E	E	LP, T	Upchurch *et al*. (1999)
Antarctica, Shackleton Ice Shelf	P	LC	68°S	112°E	E	LP, T	Upchurch *et al*. (1999)
Antarctica, Cape Carr	P	LC	67.5°S	150°E	E	LP, T	Upchurch *et al*. (1999)
Antarctica, Vega Island	P	LC	55°S	44°W	E	LP, T	Upchurch *et al*. (1999)
Australia, Gippsland Basin (Victoria)	P	LC	68°S	118°E	E	LP, T	Upchurch *et al*. (1999)
Australia, Gippsland Basin	P	LC	68°S	117°E	E	LP, T	Upchurch *et al*. (1999)
New Zealand, Kaitangata, Site L46	P	LC	81°S	155°E	E	LP, T	Upchurch *et al*. (1999)
New Zealand, Lovell's Flat, Site L214	P	LC	79°S	157°E	E	LP, T	Upchurch *et al*. (1999)
New Zealand, Morley Area	P	LC	77°S	158°E	E	LP, T	Upchurch *et al*. (1999)
New Zealand, Dunedin, Site L178	P	LC	75°S	159°E	E	LP, T	Upchurch *et al*. (1999)
New Zealand, Shag Point, Site L170	P	LC	73°S	160°E	E	LP, T	Upchurch *et al*. (1999)
New Zealand, Otago, Sites L289–291	P	LC	69°S	165°E	E	LP, T	Upchurch *et al*. (1999)
New Zealand, Pitt Island	P	LC	67°S	170°E	E	LP, T	Upchurch *et al*. (1999)
Western Australia	P	EC	50–70°S	75–105°W	E	NLR	Dettmann (1989) and Dettman *et al*. (1992)
Eastern India	P	EC	55–60°S	25–60°E	E	NLR	Dettmann (1989) and Dettman *et al*. (1992)

Fossil type: L, leaves; W, wood; P, pollen; C, dispersed leaf cuticles.
Age: EC, Early Cretaceous; LC, Late Cretaceous.
Leaf habit: E, evergreen; D, deciduous; M, mixed.

is the reduction in radial cell diameter across a growth ring relative to the maximum cell size, and PL the number of latewood cells as a percentage of the total cells in a ring (Creber & Chaloner, 1984). We note that environmental conditions experienced at the growth site (e.g. hot or cold, wet or dry), the position of the wood within the tree (branch or trunk) and the light regime at high latitude may also influence RMI and therefore our estimate of LL (Falcon-Lang, 2005). However, modern datasets obtained from branch and trunk, damaged and undamaged trees, and variations with respect to altitude and latitude, suggest that these factors only produce minor variation to the underlying genetic signal produced (Harland, 2005).

For each sample, 10 files of cells were measured across all rings that were more than 30 cells wide, and mean values derived per sample. Rings under 30 cells wide produce anomalously high values of latewood and were not used for this reason. Between one and eight rings were measured per sample. The RMI of each modern conifer genus was plotted against its known LL and the following logarithmic regression relationship determined:

$$\mathrm{RMI} = -10.28 \ln(\mathrm{LL}) + 36.228, \qquad (10)$$

($r^2 = 0.70$, $P < 0.001$).

Permineralized fossil conifer woods from trees growing at a palaeolatitude of around 75°N during the mid-Cretaceous (Aptian/Albian) in Svalbard (Arctic Norway) were analysed to estimate LL. A total of nine fossil conifer morpho-taxa were identified: *Araucariopitys*, *Protocedroxylon*, *Piceoxylon*, *Laricioxylon*, *Cedroxylon*, *Xenoxylon*, *Taxodioxylon*, *Cupressinoxylon* and *Juniperoxylon*. For each, the RMI was calculated using the same technique as for modern wood and LL estimated from the inverse of Eqn (10) ($r^2 = 0.64$, $P < 0.001$).

We estimated LL of mid-Cretaceous fossil conifer woods from the late Albian Triton Point Formation on S.E. Alexander Island, Antarctica, from published measurements of PL values (Falcon-Lang & Cantrill, 2000). These originated from forests growing at palaeolatitudes of 75°S. PL values measured in identified fossil

wood specimens reported by these authors were: *Araucarioxylon* (24.6 PL), *Araucariopitys* (26.05 PL), *Podocarpoxylon* specimen 1 (22.45 PL), *Podocarpoxylon* specimen 2 (19.1 PL), *Taxodioxylon* (49.75 PL). LL was estimated by inverting the regression relationship between PL and LL given by Falcon-Lang (2000b) ($r^2 = 0.86$, $P < 0.001$) to give

$$\mathrm{LL} = 12(\mathrm{PL} - 54.46)/ - 4.312. \quad (11)$$

Results and discussion

Simulated Cretaceous biogeography and qualitative biome reconstructions

Simulated biogeography of Cretaceous polar forest biomes is shown in Fig. 3. Northern and Southern hemispheres clearly differ in the extent of each biome (Fig. 3c and d) although moving polewards both hemispheres show a region of predominantly evergreen forest succeeded by a belt of deciduous forest at around 50° or 60° of latitude. However, a clear transition zone of mixed forest in the Northern Hemisphere is absent from the Southern Hemisphere, or at least is not resolved by the 3.75° grid spacing used here. Polewards of around 80°S in Antarctica, the belt of deciduous trees gives way to another continental region of evergreen forest with relatively short LLs (12–18 months), compared with the longer LLs (48–96 months) for the more temperate coastal Antarctic evergreen forests.

Reconstructed biome types (Table 1, Fig. 3e and f) provide an independent test of our model simulations. The comparison shows broad agreement between observed and simulated biomes, particularly in the northern hemisphere. Early and Late Cretaceous fossil plant assemblages from high-latitude sites of northern Alaska and Russia contain conifer groups that were probably deciduous, with foliage comparable with that of modern species within the Cupressaceae (e.g. *Metasequoia* and *Taxodium*) (Spicer & Parrish, 1986; Herman, 1994). In agreement with these observations, we predict either deciduous or mixed forests. At other northern high-latitude localities, where we predict mixed conifer forests, qualitative interpretation of fossil floras suggests that these deciduous plant remains are associated with microphyllous conifers like *Brachyphyllum* and cupressaceous

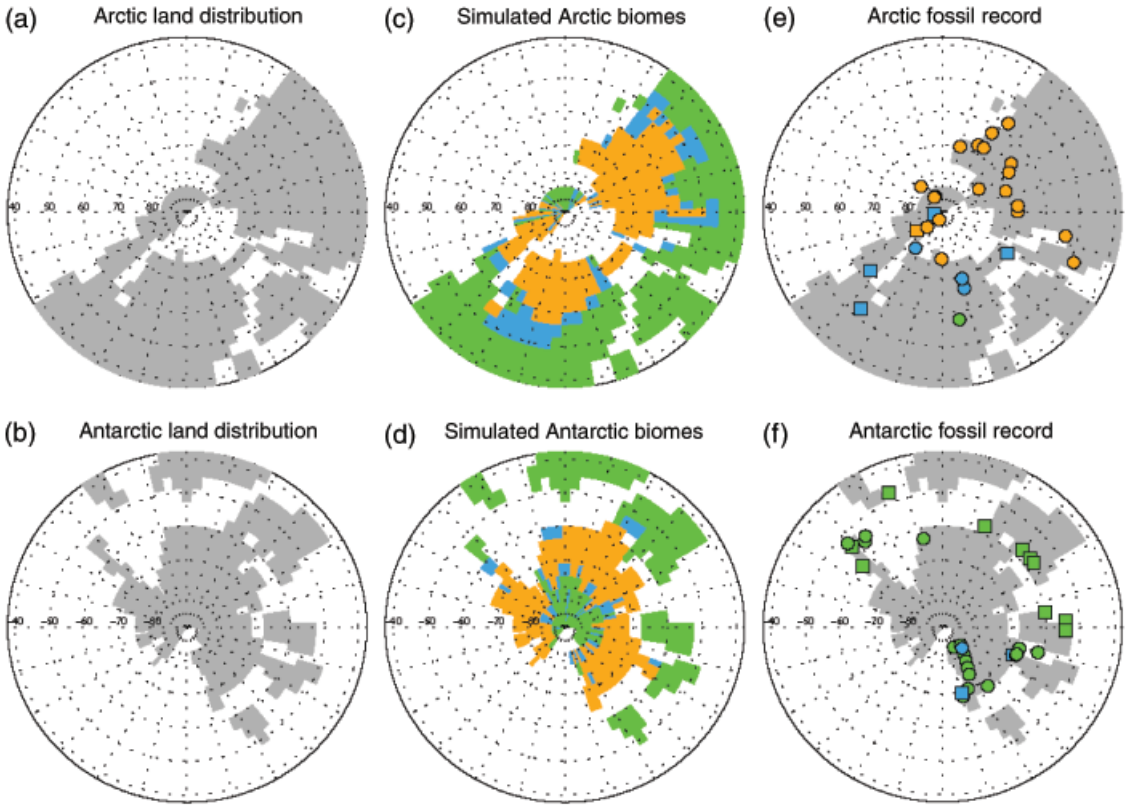

Fig. 3 Simulated and reconstructed biomes of Cretaceous polar conifer forests. (a) and (b) Land-sea mask as used in the general circulation model simulations, for the northern and southern high latitudes, respectively. (c) and (d) Simulated biomes, (e) and (f) biome-type reconstructed from the fossil record (see Table 1 for details). Symbols: squares Early Cretaceous, circles records from the late Cretaceous. Colour codes for (c–e): green, evergreen forest; orange, deciduous forest; blue, mixed forest.

forms that were probably evergreen, suggesting a mixed forest canopy (Upchurch *et al.*, 1999).

Southern Hemisphere Cretaceous pollen records at sites in southern Australia, South America and India are dominated by araucarian, podocarp and taxodiaceae conifers (Archangelsky, 1963; Douglas & Williams, 1982; Dettmann, 1989, 1992), characterized today by leaves with long LLs, in agreement with our simulations. From Antarctica the data are sparser, but show clearly that evergreen forests occurred on the Antarctic Peninsula and around the eastern margins (Dettmann, 1989; Upchurch & Askin, 1990; Parrish *et al.*, 1998; Falcon-Lang & Cantrill, 2001a, b). Three Early Cretaceous sites provide evidence for a mixture of evergreen and deciduous trees in New Zealand (Table 1), at that time adjacent to the Antarctic landmass, and these generally correspond with the simulated occurrence of these forests, although this region appears to have been occupied predominantly by evergreens in the Late Cretaceous.

Fossil data from Antarctica are all from marginal areas, at the edge of the present-day ice sheet, and give an evergreen or mixed forest signal matching the simulated forest distribution (Fig. 3; Table 1). We also simulate an extensive area of deciduous forest between 60 and 80°S on the Antarctic continent with a central core of evergreen forest at the pole. At present, however, there is no fossil evidence to test the validity of this result. We note that many Southern Hemisphere conifer taxa, like *Araucaria* and the podocarps, are evergreen today but are restricted in their southerly extent. In the Cretaceous, the pool of deciduous taxa available for forming deciduous forests was also severely restricted to *Ginkgo* and some Cupressaceae conifer types that might have been deciduous (Douglas & Williams, 1982). It is also conceivable that fire-specific adaptations, such as the fire-activated serotinous cones of the modern-day Jack pine *Pinus banksiana*, could have led to trees of longer LL having a greater effective colonization capacity than considered here.

A general problem with current GCM simulations of ancient greenhouse conditions is their tendency to predict high latitudes that are too cold relative to proxy climate indices (Barron *et al.*, 1995; Schmidt & Mysak, 1996; Valdes *et al.*, 1996; Hotinski & Toggweiler, 2003). To assess the extent of this problem for the HadAM3 simulations, we made a site-by-site comparison of temperature reconstructed from terrestrial proxies (plant physiognomy, plant and vertebrate NLRs, and vertebrate oxygen isotopes) with those derived from the HadAM3 simulation. The comparison is necessarily confined to mean annual temperature, because of the paucity of proxy evidence for the coldest month. Nevertheless, we find an average cold bias in the model of −8 °C for all Arctic localities, and −9 °C for those polewards of 70° latitude (Fig. 4). Antarctic sites are colder still, with corresponding biases of −13 °C and −14 °C (Fig. 4). The presence of frost-intolerant crocodilians at high latitudes in both hemispheres (Markwick, 1998) suggests that the very low subzero temperatures predicted by the GCM are driving the observed bias.

To investigate the influence of a high-latitude climate with a cool bias on projected forest distributions we performed a sensitivity analysis, repeating the simulations with the 3 coldest months of the Antarctic winter warmed by 10 °C or 20 °C, and those of the Arctic winter by 5 °C or 10 °C. Note that even with the larger increases, subzero winter minimum temperatures still occur in both the Arctic and the Antarctic, with small regions of subzero annual mean temperature remaining in each. The adjusted temperatures are therefore still consistent with fossil evidence of frost damage to trees (e.g. Falcon-Lang *et al.*, 2001a, b, 2004), localized sea-ice (Frakes & Francis, 1988) and small continental glaciers (Spicer & Parrish, 1986). In the absence of proxy data to the contrary, we made no changes to seasonal precipitation patterns. Results for Antarctica (Fig. 5a–c) indicate that a wintertime warming of 10 °C doubles the coverage of evergreen polar forests (from 3.3×10^6 to 6.6×10^6 km^2), particularly in West Antarctica, which experiences the moderating climatic influence of the oceans (Fig. 5b). Elsewhere on the continent, winter temperatures remain much colder; and evergreen forests only colonize these areas extensively with 20 °C of warming, reaching a total area of 15.9×10^6 km^2.

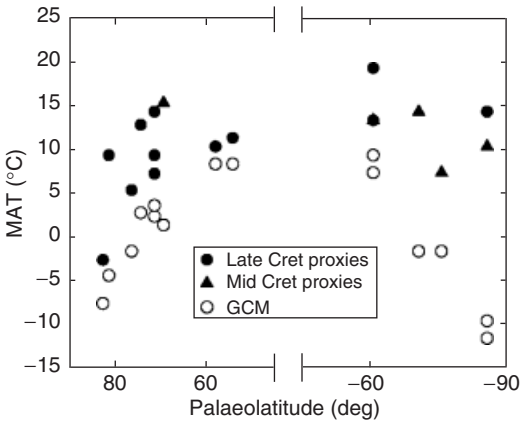

Fig. 4 Cretaceous continental latitudinal mean annual temperature (MAT) gradient inferred from fossil evidence and simulated by the Hadley Centre GCM. Data for the Northern Hemisphere sites from: Wolfe & Upchurch (1987), Herman & Spicer (1996), Tarduno *et al.* (1998), Amiot *et al.* (2004), Jenkyns *et al.* (2004); Southern Hemisphere sites: Parrish *et al.* (1991), Dettmann *et al.* (1992), Cantrill (1995), Parrish *et al.* (1998), Hayes (1999), Kennedy *et al.* (2002), and Francis & Poole (2002).

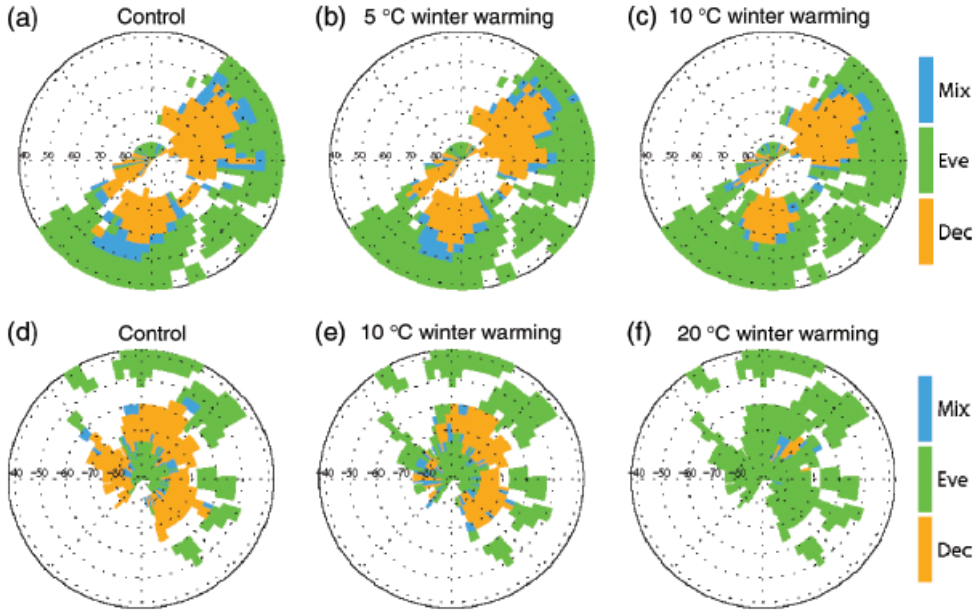

Fig. 5 Sensitivity of simulated polar forest biome distributions to the Cretaceous land surface climatology. Simulated Arctic biome distributions with the control climate (a), and the effect of +5 °C (b) and +10 °C (c) winter warming. Simulated Antarctic biome distributions with the control climate (a), and the effect of +10 °C (b) and +20 °C (c) winter warming.

Corresponding sensitivity experiments for the Arctic, with a winter warming of 5 °C or 10 °C showed the general insensitivity of the simulated biome distributions (Fig. 5a–c). Cover of the deciduous biome decreased from the control run of 12.0×10^6–11.8×10^6 and to $9.3 \times 10^6\,km^2$ with 5 °C and 10 °C of winter warming, respectively. Even though this result emerges in part from the smaller imposed warming, it, nevertheless, indicates the robust persistence of the northern high-latitude deciduous biome.

A second set of sensitivity runs was performed to allow for the possibility that the GCM underestimates the precipitation in the Arctic during the Cretaceous. With precipitation doubled, the area occupied by the deciduous biome north of 60°N decreased from 12.0×10^6 to $9.8 \times 10^6\,km^2$, with the coverage of mixed forest almost doubling, from 1.8×10^6 to $3.5 \times 10^6\,km^2$. This result is consistent with the mechanistic analysis presented in the following subsection; by lengthening the fire return interval, the enhanced precipitation favours evergreens in these regions. Overall, however, the patterns remained similar to those in the control integration.

Overall, our sensitivity analyses argue strongly that, given an appropriate land surface climatology, the coupled USCM and forest dynamics scheme adequately reproduce patterns of polar forest biogeography seen in the fossil record. The process-based nature of the model allows investigation of the ecological and climatic mechanisms driving the simulated patterns.

Mechanistic analysis of simulated Cretaceous polar forest LL across latitudinal transects

Our regional-scale simulations and sensitivity analyses (Figs 3 and 5) indicate a crucial role for climate in determining the biogeography of polar forest LL. To investigate climate–LL interactions, we analyse a latitudinal transect for a Cretaceous climate in the Northern Hemisphere (60–90°N), stretching from western Canada to Alaska. Simulations account for nine competing LLs, but for ease of interpretation and to illustrate variation in ecological properties, we examine two dominant LLs for deciduous (LL = 6 months) and evergreen (LL = 96 months) trees (Fig. 6). The transect, therefore, focuses on variation in climate and disturbance, providing a generally applicable exemplar for explaining why evergreen and deciduous trees dominate at different latitudes in our simulations.

Both MAT and MAP decline along the transect (Fig. 6a and b), causing a decrease in the fire return interval from 1200 to 50 years (Fig. 6c). Evergreens dominate in the temperate climate of western Canada (60–70°N), where fire return intervals are relatively long, whereas deciduous trees dominate in the higher latitudes (Fig. 6d), where a drier climate leads to a shorter fire return interval. Because the latitudinal decline in NPP is similar for both LLs (Fig. 6e), in agreement with experimental and field observations (Hollinger, 1992; Royer *et al.*, 2003, 2005; Dungan *et al.*, 2004), it cannot explain the transition from evergreen to deciduous forest. In-

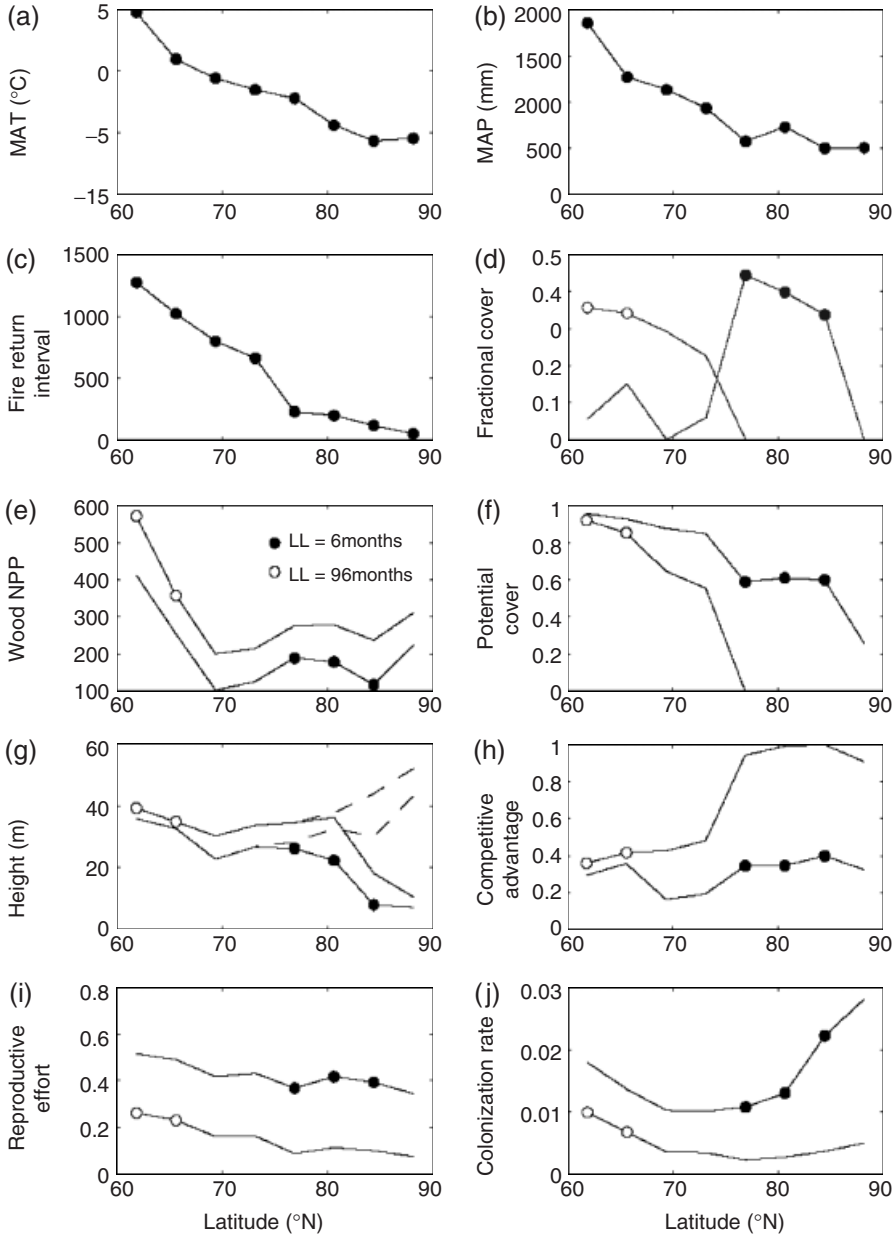

Fig. 6 Climate and ecological traits of trees with different leaf lifespan (LL) along an exemplar latitudinal transect from western Canada to Alaska. Solid symbols indicate sites at which that LL is dominant along the transect. Changes in mean annual temperature (MAT) (a), mean annual precipitation (MAP) (b), fire return interval ($1/\gamma$) (c), fractional cover for each LL (d), wood net primary production (NPP, $g\,C\,m^{-2}\,yr^{-1}$) (e), potential cover (f), height attained in the space of a fire return interval (g), dashed lines show the height that would be attained without disturbance by fire, competitive advantage defined as $1-\sum_{j=1}^{n} c_{ij}\,v_j$ (h), (h), reproductive effort (i) and colonization rate (j) along the transect. See text for further details.

stead, the explanation lies in a sequence of secondary succession, reflecting a trade-off with increasing LL between the ability to compete for light and colonize after disturbance.

The long fire return interval at lower latitudes (Fig. 6c) allows potential cover to approach 1.0 for evergreen and deciduous trees (Fig. 6f), because both slow and fast colonizers would have sufficient time to spread throughout the gridbox in the absence of competition. However, this climatic potential is modified as a result of competition for light, with the height advantage (Fig. 6g) of evergreens promoting a significant competitive advantage (Fig. 6h). Trees with longer LLs grow taller because their lower stomatal conductance to water

vapour (Reich *et al*., 1999; Wright *et al*., 2004) can be matched by a lower trunk conductance, while still avoiding desiccation of leaves in the treetop (Whitehead *et al*., 1984; Osborne & Beerling, 2002b; Koch *et al*., 2004). The low trunk conductance of tall trees results from a high ratio of length to cross-sectional area in sapwood, which transports water through the trunk. Simulated tree heights of 40 m (Fig. 6g) are well within the limits reached by today's forests of the humid temperate climate of western Canada, and entirely compatible with estimates of 40 m for a fossilized deciduous forest of Eocene age (*Metasequoia* sp.) from the Canadian High Arctic (Williams *et al*., 2003).

As the fire return interval shortens with increasing latitude, the potential cover of evergreen trees is greatly diminished (Fig. 6f) because their reproductive effort is low relative to deciduous trees (Fig. 6i), and colonization rate declines rapidly (Fig. 6j) as a consequence of this and falling NPP (Fig. 6e). At latitudes of 78°N and higher, the colonization rate of evergreens is insufficient for recovery after fire disturbance, preventing the establishment of populations and their persistence at high latitudes (potential cover = 0). In effect, deciduous trees establish more rapidly and effectively than evergreens, and this is a critical determinant of success in a disturbed environment. We emphasize that the absence of evergreens with long LL from these deciduous high-latitude forests does not preclude the occurrence of evergreens with shorter LL. In fact, forests with a range of LLs are an emergent property of our dynamic vegetation model simulations.

We have focused on fire as the mechanism of disturbance because it is the principal determinant of boreal and subboreal forest composition in the present day (Johnson, 1992; Frelich, 2002). Furthermore, evidence of wildfire in the Cretaceous polar forests, in the form of charcoal, is abundant in the Arctic (e.g. Falcon-Lang *et al*., 2004), and has been discovered in the Antarctic (Eklund *et al*., 2004). Other sources of disturbance could, however, easily be incorporated into the model.

Simulated and observed LLs of Antarctic and high Arctic polar forests

We sought to unite model predictions of LL with observations on fossil wood for two case studies on high northern (Svalbard in the high Arctic) and southern (Alexander Island on the Antarctic Peninsula) latitude sites. Analysing the fossil remains of polar forests from these two sites provides information about the actual range of LL in these ecosystems, as well as a direct quantitative test of model accuracy. Examination of the two specific localities shifts the focus from latitudinal gradients of climate to variation in LL.

From Svalbard, LL values estimated from fossil woods fell into two distinct groups, with LL either less ($n = 4$) or greater ($n = 8$) than 18 months (Table 2). In comparison, we simulate a bimodal distribution of LLs at this locality, with peaks of fractional cover at 6 months in the deciduous and 48 months in the evergreen range (Fig. 7a). This result compares favourably with the two groups of LL estimated using fossils, which had mean values of 8 and 50 months, respectively (Table 2; Fig. 7a). Two independent lines of evidence therefore indicate that Svalbard was populated by a mixed forest biome in the Early Cretaceous.

On Alexander Island, Antarctica, our reinterpretation of a published report of PL for a range of wood taxa (Falcon-Lang & Cantrill, 2000) (Eqn (11)) gives a different pattern, with only a single taxon having a short LL, and four taxa with LL of 79 months or more (Table 2). The range of high LLs at this site are in agreement with complementary approaches used to infer leaf habit from fossils, especially the presence of leaf traces, leaf taphonomy and leaf physiognomy (Falcon-Lang & Cantrill, 2000). The wood taxa used in this analysis closely

Table 2 Estimated leaf lifespan (LL ± upper and lower 95% confidence limits) of fossil woods from the European high Arctic (Svalbard) and Alexander Island, Antarctica

Site	Wood taxon	Estimated LL (± 95% range) (months)
Svalbard	*Laricioxylon* (species A)	11 (5.5–18.2)
	Laricioxylon (species B)	5 (2.1–9.2)
	Taxodioxylon (species C)	13 (6.7–21.1)
	Protocedroxylon	18 (9.8–27.9)
	Mean	**11.8 (5.9–19.4)**
	Araucariopitys	57 (38.7–75.9)
	Piceoxylon	35 (21.7–49.6)
	Cedroxylon	76 (54.3–97.7)
	Xenoxylon	69 (48.5–89.7)
	Taxodioxylon	42 (26.9–58.2)
	Taxodioxylon (species B)	100 (75.0–124.5)
	Cupressinoxylon	48 (31.6–65.3)
	Juniperoxylon	41 (26.2–57.0)
	Mean	**58.5 (40.0–77.7)**
Alexander Island	*Taxodioxylon*	13 (6.7–21.1)
	Araucarioxylon	83 (60.2–105.6)
	Araucariopitys	79 (56.8–101.1)
	Podocarpoxylon (morphospecies 1)	89 (65.4–112.3)
	Podocarpoxylon (morphospecies 2)	98 (73.2122.3)
	Mean	**87.3 (63.9–110.4)**

mirror the foliage fossil record at the same locality (Cantrill & Falcon-Lang, 2001). Model simulations for Alexander Island indicate a predominance of evergreen trees with LL > 48 months, and a minor component of deciduous trees with LL = 9 months (Fig. 7b).

Estimated and simulated LLs from both Arctic and Antarctic sites are in close quantitative agreement, an agreement that provides strong validation for the coupled USCM and forest dynamics scheme. Climatic differences and ensuing disturbance regimes between the sites underpin their contrasting forest compositions. In Svalbard, a cool, dry climate (unadjusted MAT = 4 °C, MAP = 600 mm) yields a fire return interval of 80 years, leaving insufficient time for evergreen trees with long LL to achieve a high potential cover (Fig. 8a, Eqn (6)) as colonization rate declines sharply with LL (Fig. 8b). This results from a decrease in the partitioning of resources to reproduction with LL (Fig. 8c, Eqns (2) and (3)), rather than a change in NPP with LL (Fig. 8d). Potential cover of deciduous trees with short LLs is also constrained by colonization rate (Fig. 8a and b), as a consequence of decreasing reproductive effort (Fig. 8c) and NPP (Fig. 8d). The net outcome is the elimination of trees with very short or very long LLs by fire (Fig. 7a). The most successful trees, in terms of cover, are those with an LL ensuring they attain reasonable potential cover while retaining a significant competitive advantage (Fig. 8e). Competitive advantage mirrors height (Fig. 8f, Eqn (4)), which is inversely related to the transpiration rate. Transpiration peaks with an LL of 18 months because the short-lived evergreen canopy attains both a high LAI in combination with a high stomatal conductance. The mixture of trees at this locality reflects the complex interplay between climate, LL and the ecological processes involved in succession.

On Alexander Island the warm, wet climate (GCM MAT = 6.9 °C, MAP = 1378 mm) lengthens the fire return interval to 368 years, ensuring that trees with all LLs have a high potential cover (Fig. 8a). In support of such low fire frequencies, we note that long tree ring sequences of fossil woods from the same Antarctic site indicate tree longevities of at least 180 years (Chapman, 1994; Falcon-Lang & Cantrill, 2000). Consequently, forest composition is determined by competition for light (Fig. 8e) (i.e. by the potential height of trees with each LL) (Fig. 8f). Without frequent disturbance, the small height advantage of slow colonizing trees with long LLs (> 48 months) is enough to tip the balance decisively in their favour, leaving only ~ 10% of the vegetated area occupied by deciduous trees (Fig. 7b). The marked contrast in forest composition at this locality with that at Svalbard highlights the critical importance of vegetation dynamics for shaping community composition in the postdisturbance environment. Disturbances other than fire, such as wind-throw, volcanism, herbivory or flooding, would amplify these effects.

Conclusion

Palaeobotanical interpretation of polar forests has long hinged on the assumption that the deciduous leaf habit was an important adaptation for tree survival in a warm, high-latitude environment (Osborne *et al.*, 2004). Recent experiments (Royer *et al.*, 2003, 2005) and the reinterpretation of Antarctic fossil floras (Falcon-Lang & Cantrill, 2001a, b) are now challenging this view. This paper presents a first attempt at an alternative interpretation of the factors controlling the biogeography of LL in polar forests that links mechanistic understanding of its functional consequences for plant resource-use and forest dynamics. An important outcome highlighted by our analyses is the crucial influence of disturbance and its interaction with LL. We recognize that there are alternative approaches to simulating fire in the natural landscape (e.g. Thonicke *et al.*,

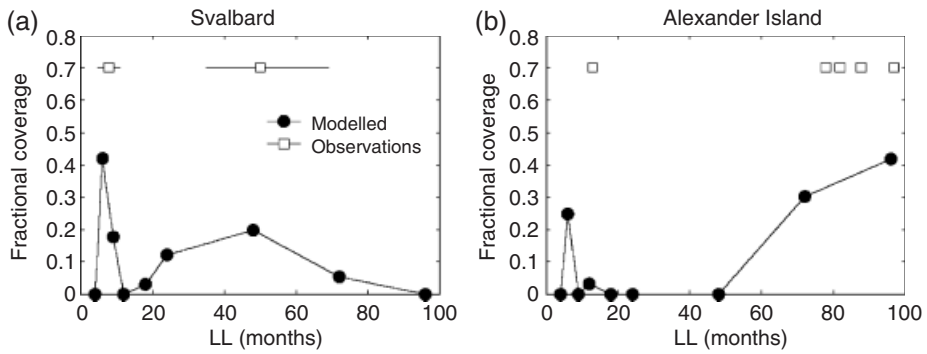

Fig. 7 Modelled and observed dominance of trees with different leaf lifespans (LLs) of the Cretaceous polar conifer forests of Svalbard (a) and Alexander Island, Antarctica (b). For Svalbard, the mean and range of the observed deciduous LLs are shown; for the evergreens, the mean and interquartile range is indicated. Individual estimates of LL are shown for Alexander Island.

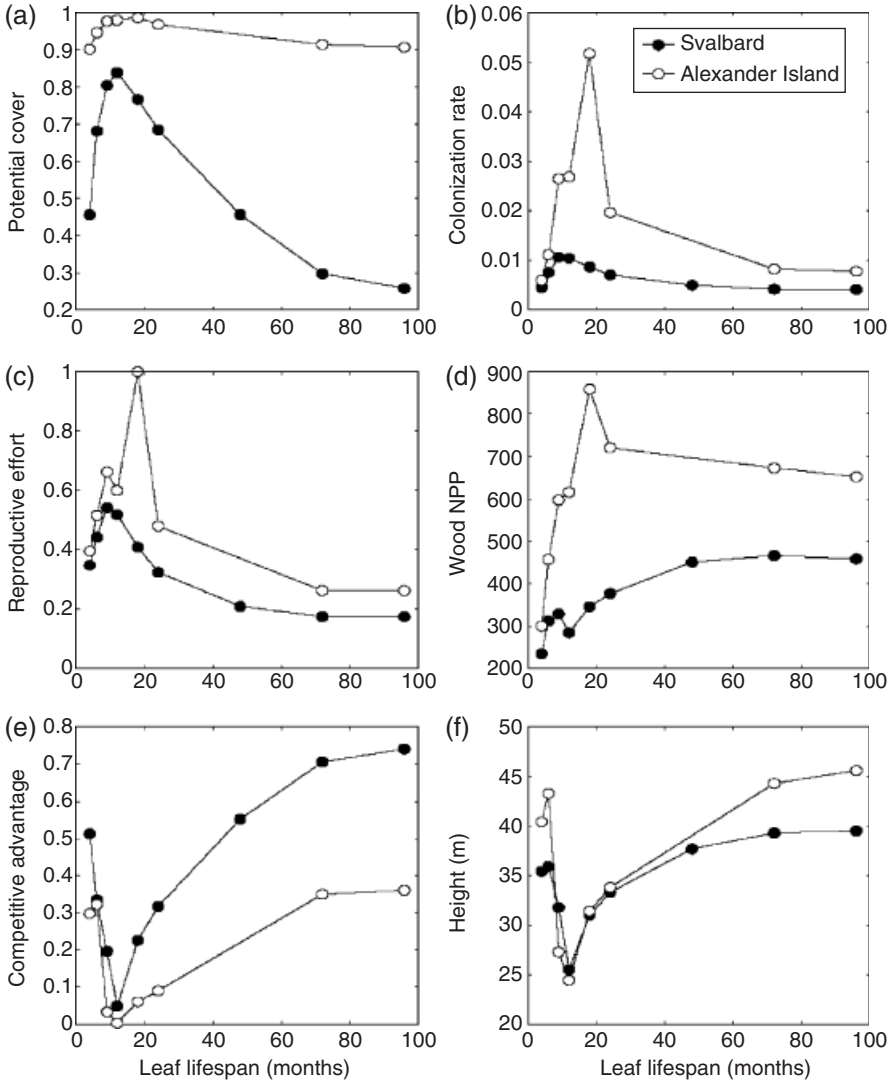

Fig. 8 The simulated influence of leaf lifespan (LL) on the ecological properties of Cretaceous polar forests at Svalbard (European high Arctic) and Alexander Island, Antarctica. The graphs illustrate the effect of LL on potential cover (a), colonization rate (b), reproductive effort (c), wood net primary production (NPP, $g C m^{-2} yr^{-1}$) (d), competitive advantage (e) and height (f). See text for details.

2001) and to describing the relationship between LL and the process of succession (e.g. Shugart & Smith, 1996; Hall & Hollinger, 2000; Bugmann, 2001). Our work, therefore, represents the first step towards developing an alternative perspective on the significance that LL holds for polar forest biogeography.

Acknowledgements

We thank Dana Royer, Ian Woodward, Howard Falcon-Lang and an anonymous reviewer for helpful comments on the manuscript. D. J. B. and J. E. F. gratefully acknowledge funding of this work through the NERC (NER/A/S/2001/00435). MH gratefully acknowledges funding through the NERC studentship (NERC/S/J/2002/10896) and V. W. a Worldwide University Network (WUN) research studentship. J. E. F. thanks L. A. Frakes (University of Adelaide) and the Australian Research Council for the opportunity to collect wood on Svalbard and C. Day for field assistance.

References

Amiot R, Lecuyer C, Buffetaut E *et al*. (2004) Latitudinal temperature gradient during the Cretaceous Upper Campanian-Middle Maastrichtian: $\delta^{18}O$ record of continental vertebrates. *Earth and Planetary Science Letters*, **226**, 255–272.

Archangelsky S (1963) A new Mesozoic flora from Tico, Santa Cruz province, Argentina. *Bulletin of the British Museum (Natural History), Geology*, **8**, 47–92.

Axelrod DI (1966) Origin of deciduous and evergreen habits in temperate forests. *Evolution*, **20**, 1–15.

Axelrod DI (1984) An interpretation of Cretaceous and Tertiary biota in polar regions. *Palaeogeography, Palaeoclimatology, Palaeoecology*, **45**, 105–147.

Barron EJ, Fawcett PJ, Peterson WH *et al*. (1995) A 'simulation' of the mid-cretaceous. *Paleoceanography*, **10**, 953–962.

Bazzaz FA (1979) The physiological ecology of plant succession. *Annual Review of Ecological Systematics*, **10**, 351–371.

Bazzaz FA (1996) *Plants in Changing Environments. Linking Physiological, Population, and Community Ecology*. Cambridge University Press, Cambridge.

Beerling DJ, Osborne CP (2002) Physiological ecology of Mesozoic polar forests in a high CO_2 environment. *Annals of Botany*, **89**, 329–339.

Beerling DJ, Woodward FI (2001) *Vegetation and the Terrestrial Carbon Cycle. Modelling the First 400 Million Years*. Cambridge University Press, Cambridge.

Boyd A (1994) Some limitations in using leaf physiognomic data as a precise method for determining palaeoclimates with an example from the Late Cretaceous Pautut Flora of West Greenland. *Palaeogeography, Palaeoclimatology, Palaeoecology*, **112**, 261–278.

Bugmann H (2001) A review of forest gap models. *Climatic Change*, **51**, 259–305.

Cantrill DJ (1995) The occurrence of a fern *Hausmannia* Dunker (Dipteridaceae) in the Cretaceous of Alexander Island, Antarctica. *Alcheringa*, **19**, 243–254.

Cantrill DJ, Falcon-Lang HJ (2001) Cretaceous (Late Albian) Coniferales of Alexander Island, Antarctica. part 2: leaves, reproductive organs and roots. *Review of Palaeobotany and Palynology*, **115**, 119–145.

Chaloner WG, Creber GT (1990) Do fossil plants give a climatic signal? *Journal of the Geological Society, London*, **147**, 343–350.

Chaney RW (1947) Tertiary centers and migration routes. *Ecological Monographs*, **17**, 139–148.

Chanzy A, Bruckler L (1993) Significance of soil surface moisture with respect to daily bare soil evaporation. *Water Resources Research*, **29**, 1113–1125.

Chapman JL (1994) Distinguishing internal developmental characteristics from external palaeoenvironmental effects in fossil wood. *Review of Palaeobotany and Palynology*, **81**, 19–32.

Cox PM (2001) *Description of the 'TRIFFID' dynamic global vegetation model*. Hadley Centre Technical Note, 24, 16pp.

Crane PR (1987) Vegetational consequences of angiosperm diversification. In: *The Origins of Angiosperms and their Biological Consequences* (eds Friis EM, Chaloner WG, Crane PR), pp. 107–144. Cambridge University Press, Cambridge.

Creber GT, Chaloner WG (1984) Influence of environmental factors on the wood structure of living and fossil trees. *The Botanical Review*, **50**, 357–448.

Creber GT, Chaloner WG (1985) Tree growth in the Mesozoic and Early Tertiary and the reconstruction of palaeoclimates. *Palaeogeography, Palaeoclimatology, Palaeoecology*, **52**, 35–60.

Crowley TJ, Berner RA (2001) CO_2 and climate change. *Science*, **292**, 870–872.

DeFries R, Hansen M, Townshend JRG *et al*. (2000a) *Continuous Fields 1 km Tree Cover*. The Global Land Cover Facility, College Park, MD.

DeFries R, Hansen M, Townshend JRG *et al*. (2000b) A new global 1 km data set of percent tree cover derived from remote sensing. *Global Change Biology*, **6**, 247–254.

DePury DGG, Farquhar GD (1997) Simple scaling of photosynthesis from leaves to canopies without errors of big-leaf models. *Plant, Cell and Environment*, **20**, 537–557.

Dettmann ME (1989) Antarctica: Cretaceous cradle of austral temperate rainforests? *Geological Society Special Publication*, **42**, 89–105.

Dettmann ME, Molnar RE, Douglas JG *et al*. (1992) Australian Cretaceous terrestrial fauna and floras: biostratigraphic and biogeographic implications. *Cretaceous Research*, **13**, 207–262.

Didier L (2001) Invasion patterns of European larch and Swiss stone pine in subalpine pastures in the French Alps. *Forest Ecology and Management*, **145**, 67–77.

Doležal J, Ishii H, Vetrova VP *et al*. (2004) Tree growth and competition in a *Betula platyphylla-Larix cajanderi* post-fire forest in Central Kamchatka. *Annals of Botany*, **94**, 333–343.

Douglas JG, Williams GE (1982) Southern polar forests: the early Cretaceous floras of Victoria and their palaeoclimatic significance. *Palaeogeography, Palaeoclimatology, Palaeoecology*, **39**, 171–185.

Dungan RJ, Whiteheard D, McGlone M *et al*. (2004) Simulated carbon uptake for a canopy of two broadleaved tree species with contrasting leaf habit. *Functional Ecology*, **18**, 34–42.

Dutton AL, Lohmann KC, Zinsmeister WJ (2002) Stable isotope and minor element proxies for Eocene climate of Seymour Island, Antarctica. *Paleoceanography*, **17**, 1016, doi: 10.1029/2000PA000593.

Eklund HE, Cantrill DJ, Francis JE (2004) Late Cretaceous plant mesofossils from Table Nunatak, Antarctica. *Cretaceous Research*, **25**, 211–228.

Enquist BJ, Brown JH, West GB (1998) Allometric scaling of plant energetics and population density. *Nature*, **395**, 163–165.

Farquhar GD, von Caemmerer S, Berry JA (1980) A biochemical model of photosynthetic CO_2 assimilation in leaves of C_3 species. *Planta*, **149**, 78–90.

Falcon-Lang HJ (2000a) A method to distinguish between woods produced by evergreen and deciduous coniferopsids on the basis of growth ring anatomy: a new palaeoecological tool. *Palaeontology*, **43**, 785–793.

Falcon-Lang HJ (2000b) The relationship between leaf longevity and growth ring markedness in modern conifer woods and its implications for palaeoclimatic studies. *Palaeogeography, Palaeoclimatology, Palaeoecology*, **160**, 317–328.

Falcon-Lang HJ (2005) Intra-tree variability in wood anatomy, and its implications for fossil wood systematics and palaeoclimatic datasets. *Palaeontology*, **48**, 171–183.

Falcon-Lang HJ, Cantrill DJ (2000) Cretaceous (Late Albian) coniferales of Alexander Island, Antarctica: Wood taxonomy: a quantitative approach. *Review of Palaeobotany and Palynology*, **111**, 1–17.

Falcon-Lang HJ, Cantrill DJ (2001a) Leaf phenology of some mid-Cretaceous polar forests, Alexander Island, Antarctica. *Geological Magazine*, **138**, 39–52.

Falcon-Lang HJ, Cantrill DJ (2001b) Gymnosperm woods from the Cretaceous (mid-Aptian) Cerro Negro Formation, Byers Peninsula, Livingston Island, Antarctica: the arborescent vegetation of a volcanic arc. *Cretaceous Research*, **22**, 277–293.

Falcon-Lang HJ, MacRae RA, Csank AZ (2004) Palaeoecology of Late Cretaceous polar vegetation preserved in the Hansen Point Volcanics, NW Ellesmere Island, Canada. *Palaeogeography, Palaeoclimatology, Palaeoecology*, **212**, 45–64.

Frakes LA, Francis JE (1988) A guide to Phanerozoic cold polar climates from high-latitude ice-rafting in the Cretaceous. *Nature*, **333**, 547–549.

Francis JE, Poole I (2002) Cretaceous and early Tertiary climates of Antarctica: evidence from fossil wood. *Palaeogeography, Palaeoclimatology, Palaeoecology*, **182**, 47–64.

Frelich LE (2002) *Forest Dynamics and Disturbance Regimes. Studies from Temperate Evergreen–Deciduous Forests*. Cambridge University Press, Cambridge.

Givnish TJ (2002) Adaptive significance of evergreen vs. deciduous leaves: solving the triple paradox. *Silva Fennica*, **36**, 703–743.

Grime JP (2001) *Plant Strategies, Vegetation Processes, and Ecosystem Properties*. John Wiley & Sons Ltd, Chichester.

Grubb PJ (2002) Leaf form and function – towards a radical new approach. *New Phytologist*, **155**, 317–320.

Hall GMJ, Hollinger DY (2000) Simulating New Zealand forest dynamics with a generalized temperate forest gap model. *Ecological Applications*, **10**, 115–130.

Harland BM (2005) Cretaceous polar conifer forests: Composition, leaf life-span and climate significance. PhD thesis, University of Leeds, Leeds, UK.

Hayes PA (1999) *Cretaceous angiosperm leaf floras from Antarctica*. PhD thesis, University of Leeds, Leeds.

Herman A (1994) Diversity of the Cretaceous Platanoid plants of the Anadyr'-Koryak subregion in relation to climatic changes. *Stratigraphy and Geological Correlation*, **2**, 365–378.

Herman AB, Spicer RA (1996) Palaeobotanical evidence for a warm Cretaceous Arctic ocean. *Nature*, **380**, 330–333.

Hewitt CD, Mitchell JFB (1996) GCM simulations of the climate of 6 kyr BP: mean changes and interdecadal variability. *Journal of Climate*, **9**, 3505–3529.

Hickey LJ (1984) Eternal summer at 80 degrees north. *Discovery*, **17**, 17–23.

Hill RS, Scriven LJ (1995) The angiosperm–dominated woody vegetation of Antarctica – a review. *Review of Palaeobotany and Palynology*, **86**, 175–198.

Hollinger DY (1992) Leaf and simulated whole-canopy photosynthesis in 2 co-occurring tree species. *Ecology*, **73**, 1–14.

Hotinski RM, Toggweiler JR (2003) Impact of a Tethyan circumglobal passage on ocean heat transport and 'equable' climates. *Paleoceanography*, **18** doi:10.1029/2001PA000703.

Jain TB, Graham RT, Morgan P (2004) Western white pine growth relative to forest openings. *Canadian Journal of Forest Research*, **34**, 2187–2198.

Jenkyns HC, Forster A, Schouten S *et al*. (2004) High latitude temperatures in the Late Cretaceous. *Nature*, **432**, 888–892.

Johnson EA (1992) *Fire and Vegetation Dynamics: Studies from the North American Boreal Forest*. Cambridge University Press, Cambridge.

Kennedy EM, Spicer RA, Rees PM (2002) Quantitative paleoclimate estimates from Late Cretaceous and Paleocene leaf floras in the northwest of South Island, New Zealand. *Palaeogeography, Palaeoclimatology, Palaeoecology*, **184**, 321–345.

Kikuzawa K (1991) A cost–benefit analysis of leaf habit and leaf longevity of trees and their geographical pattern. *American Naturalist*, **138**, 1250–1263.

Koch GW, Sillett SC, Jennings GM *et al*. (2004) The limits to tree height. *Nature*, **428**, 851–854.

Leuning R (1995) A critical appraisal of a combined stomatal-photosynthesis model for C_3 plants. *Plant, Cell and Environment*, **18**, 339–355.

Markwick PJ (1998) Fossil crocodilians as indicators of Late Cretaceous and Cenozoic climates: implications for using palaeontological data in reconstructing palaeoclimate. *Palaeogeography, Palaeoclimatology, Palaeoecology*, **137**, 205–271.

Margolis H, Oren R, Whitehead D *et al*. (1995) Leaf area dynamics of conifer forests. In: *Ecophysiology of Coniferous Forests* (eds Smith WK, Hinkley TM), pp. 181–223. Academic Press, San Diego.

Mason HL (1947) Evolution of certain floristic associations in Western North America. *Ecological Monographs*, **17**, 201–210.

Meeson BW, Corprew FE, McManus JM *et al*. (1995) *The ISLSCP Initiative I – Global Datasets for Land-Atmosphere Models, 1987–1988*. Volumes 1–5 published on CD by NASA.

Monteith JL (1965) Evaporation and the environment. In: *The State and Movement of Water in Living Organisms* (ed Fogg CE), pp. 205–234. Cambridge University Press, New York.

Myneni RB, Nemani RR, Running SW (1997) Estimation of global leaf area index and absorped PAR using radiative transfer models. *IEEE Transactions on Geoscience and Remote Sensing*, **35**, 1380–1393.

New M, Hulme M, Jones PD (1999) Representing twentieth century space-time climate variability. I. Development of a 1961–90 mean monthly terrestrial climatology. *Journal of Climate*, **12**, 829–856.

New M, Hulme M, Jones PD (2000) Representing twentieth century space–time climate variability. II. Development of 1901–96 mean monthly grids of terrestrial surface climate. *Journal of Climate*, **13**, 2217–2238.

Osborne CP, Beerling DJ (2002a) A process-based model of conifer forest structure and function with special emphasis on leaf lifespan. *Global Biogeochemical Cycles*, **16**, 1097, doi:10.1029/2001GB001467 (2002).

Osborne CP, Beerling DJ (2002b) Sensitivity of tree growth to a high CO_2 environment: consequences for interpreting the characteristics of fossil woods from ancient 'greenhouse' worlds. *Palaeogeography, Palaeoclimatology, Palaeoecology*, **182**, 15–29.

Osborne CP, Beerling DJ (2003) The penalty of a long hot summer. Photosynthetic acclimation to high CO_2 and continuous light in 'living fossil' conifers. *Plant Physiology*, **133**, 803–812.

Osborne CP, Royer DL, Beerling DJ (2004) Adaptive role of leaf habit in extinct polar forests. *International Forestry Review*, **6**, 181–186.

Parrish JT, Spicer RA, Douglas JG *et al*. (1991) Continental climate near the Albian South Pole and comparison with the climate near the North Pole. *Geological Society of America Abstracts with Programs*, **23**, 31–34.

Parrish JT, Daniel IL, Kennedy EM (1998) Paleoclimatic significance of mid-Cretaceous floras from the Middle Clarence Valley, New Zealand. *Palaios*, **13**, 149–159.

Parton WJ, Scurlock JMO, Ojima DS *et al*. (1993) Observations and modelling of biomass and soil organic matter dynamics for the grassland biome worldwide. *Global Biogeochemical Cycles*, **7**, 785–809.

Penman HL (1948) Evaporation from open water, bare soil and grass. *Proceedings of the Royal Society, Series A*, **193**, 120–145.

Pole M, Douglas B (1999) Plant megafossils of the Upper Cretaceous Kaitangata coalfield, New Zealand. *Australian Systematic Botany*, **12**, 331–364.

Pope VD, Gallani ML, Rowntree PR *et al*. (2000) The impact of new physical parametrizations in the Hadley Centre climate model: HadAM3. *Climate Dynamics*, **16**, 123–146.

Read J, Francis J (1992) Responses of some Southern Hemisphere tree species to a prolonged dark period and their implications for high-latitude Cretaceous and Tertiary floras. *Palaeogeography, Palaeoclimatology, Palaeoecology*, **99**, 271–290.

Reich PB, Ellsworth DS, Walters MB (1998) Leaf structure (specific leaf area) modulates photosynthesis–nitrogen relations: evidence from within and across species and functional groups. *Functional Ecology*, **12**, 948–958.

Reich PB, Ellsworth DS, Walters MB *et al*. (1999) Generality of leaf trait relationships: a test across six biomes. *Ecology*, **80**, 1955–1969.

Reich PB, Walters MB, Ellsworth DS (1997) From tropics to tundra: global convergence in plant functioning. *Proceedings of the National Academy of Sciences, USA*, **94**, 13730–13734.

Royer DL, Berner RA, Montañez IP *et al*. (2004) CO_2 as a primary driver of Phanerozoic climate. *Geological Society of America Today*, **14**, 4–10.

Royer DL, Osborne CP, Beerling DJ (2003) Carbon loss by deciduous trees in a CO_2-rich ancient polar environment. *Nature*, **424**, 60–62.

Royer DL, Osborne CP, Beerling DJ (2005) Contrasting seasonal patterns of carbon gain in evergreen and deciduous trees of ancient polar forests. *Paleobiology*, **31**, 141–150.

Ryan MG, Hubbard RM, Pongracic S *et al*. (1996) Foliage, fine-root, woody-tissue and stand respiration in *Pinus radiata* in relation to nitrogen status. *Tree Physiology*, **16**, 333–343.

Schmidt GA, Mysak LA (1996) Can increased poleward oceanic heat flux explain the warm Cretaceous climate? *Paleoceanography*, **11**, 579–593.

Schulze E-D, Vygodskaya NN, Tchebakova *et al*. (2002) The Eurosiberian Transect: an introduction to the experimental region. *Tellus B*, **54**, 421–428.

Seward AC (1926) The Cretaceous plant-bearing rocks of Western Greenland. *Philosophical Transactions of the Royal Society London*, **B215**, 57–172.

Shaw RH, Pereira AR (1982) Aerodynamic roughness of a plant canopy: a numerical experiment. *Agricultural and Forestry Meteorology*, **26**, 51–65.

Shugart HH, Smith TM (1996) A review of forest patch models and their application to global change research. *Climatic Change*, **34**, 131–153.

Silvertown J, Lovett-Doust J (1993) *Introduction to Plant Population Ecology*. Blackwell Science, Oxford.

Smiley C (1976) Pre-Tertiary phytogeography and continental drift – some apparent discrepancies. In: *Historical Biogeography, Plate Tectonics and the Changing Environment* (eds Gray J, Boucot AJ), pp. 311–320. Oregon State University Press, Corvallis, Oregon.

Smith AG, Smith DG, Funnell BM (1994) *Atlas of Mesozoic and Cenozoic Coastlines*. Cambridge University Press, Cambridge.

Spicer RA, Chapman JL (1990) Climate change and the evolution of high-latitude terrestrial vegetation and flora. *Trends in Ecology and Evolution*, **5**, 279–284.

Spicer RA, Corfield RM (1992) A review of terrestrial and marine climates in the Cretaceous with implications for modelling the 'Greenhouse Earth'. *Geological Magazine*, **129**, 169–180.

Spicer RA, Parrish JT (1986) Palaeobotanical evidence for cool north polar climates in middle Cretaceous (Albian-Cenomanian) time. *Geology*, **14**, 703–706.

Tarduno JA, Brinkman DB, Renne PR *et al*. (1998) Evidence for extreme climatic warmth from Late Cretaceous arctic vertebrates. *Science*, **282**, 2241–2244.

Thonicke K, Venevsky S, Sitch S *et al*. (2001) The role of fire disturbance for global vegetation dynamics: coupling fire into a dynamic global vegetation model. *Global Ecology and Biogeography*, **10**, 661–677.

Tripati A, Zachos J, Marincovich L *et al*. (2001) Late Paleocene Arctic coastal climate inferred from molluscan stable and radiogenic isotope ratios. *Palaeogeography, Palaeoclimatology, Palaeoecology*, **170**, 101–113.

Upchurch GR, Askin RA (1989) Latest Cretaceous and earliest Tertiary dispersed cuticles from Seymour Island, Antarctica. *Antarctic Journal of the United States*, **24**, 7–10.

Upchurch GR, Wolfe JA (1993) Cretaceous vegetation of the Western Interior and adjacent regions of North America. *Geological Association of Canada Special Paper*, **39**, 243–281.

Upchurch GR, Otto-Bliesner BL, Scotese CR (1999) Terrestrial vegetation and its effects on climate during the latest Cretaceous. *Geological Society of America Special Paper*, **332**, 407–426.

Valdes PJ, Sellwood BW, Price GD (1996) Evaluating concepts of Cretaceous equability. *Palaeoclimates*, **1**, 139–159.

Weiss A, Norman JM (1985) Partitioning solar radiation into direct and diffuse, visible and near-infrared components. *Agricultural and Forestry Meteorology*, **34**, 205–213.

Whitehead D, Edwards WRN, Jarvis PG (1984) Conducting sapwood area, foliage area, and permeability in mature trees of *Picea sitchensis*, and *Pinus contorta*. *Canadian Journal of Forestry Research*, **14**, 940–947.

Williams CJ, Johnson AH, LePage BA *et al*. (2003) Reconstruction of Tertiary *Metasequoia* forests II. Structure, biomass, and productivity of Eocene floodplain forests in the Canadian high arctic. *Paleobiology*, **29**, 271–292.

Wolfe JA (1985) Distribution of major vegetation types during the Tertiary. In: *The Carbon Cycle and Atmospheric CO_2: Natural Variations, Archean to Present. Geophysical Monograph Series, Vol. 32*. (eds Sundquist ET, Broecker WS), pp. 357–375. American Geophysical Union, Washington.

Wolfe JA, Upchurch GR (1987) North American nonmarine climates and vegetation during the Late Cretaceous. *Palaeogeography, Palaeoclimatology, Palaeoecology*, **61**, 33–77.

Woodward FI, Lomas MR, Lee SE (2001) Predicting the future productivity and distribution of global vegetation. In: *Terrestrial Global Productivity* (eds Jacques R, Saugier B, Mooney H), pp. 521–541. Academic Press, New York.

Woodward FI, Smith TM (1994) Global photosynthesis and stomatal conductance: modelling controls by soils and climates. *Advances in Botanical Research*, **20**, 1–41.

Woodward FI, Smith TM, Emanuel WR (1995) A global land primary productivity and phytogeography model. *Global Biogeochemical Cycles*, **9**, 471–490.

Wright IJ, Reich PB, Westoby M *et al*. (2004) The worldwide leaf economics spectrum. *Nature*, **428**, 821–827.

Appendix A: Validation of coupled USCM

We tested the accuracy of annual LAI and NPP simulations using a database of modern observations encompassing a diverse range of LLs (4–138 months), and climatic regimes ranging from the Russian boreal zone to the Mediterranean, and Alaska to Florida (Osborne & Beerling, 2002a). We forced the model with site-average climatologies for the years 1961–1990 (New *et al*., 1999, 2000), as LL > 1 at the majority of test sites, implying the integration of interannual climate variability by canopy structure. In all simulations, the USCM was driven with a mean LL value for the dominant species at each site, and an atmospheric CO_2 concentration appropriate for the year of observation.

Simulations of LAI for conifer forests at 16 different sites, and NPP for 23 sites, both give reasonable agreement with observations (Appendix Fig. 1A, LAI $r^2 = 0.84$, $P < 0.01$, NPP $r^2 = 0.89$, $P < 0.01$). In both cases, agreement between the USCM and observations was comparable with that obtained by driving the uncoupled model with prescribed soil carbon and nitrogen values (LAI, $r^2 = 0.88$; NPP, $r^2 = 0.91$) (Osborne & Beerling, 2002a), suggesting adequate simulation of soil carbon and nitrogen cycling in a self-consistent manner. On a site-by-site basis, therefore, these results indicate the capability of the USCM to accurately simulate the structure and function of conifer forests across a wide climatic gradient from inputs of climate, LL and CO_2.

We verified regional-scale model simulations of forest properties by comparison with satellite data products: the ISLSCP global land cover dataset (Meeson *et al*., 1995), which classifies each 1° gridbox into one of 15 land surface types (water, ice, desert and 12 vegetation types); the Moderate Resolution Imaging Spectroradiometer monthly 16 km LAI dataset (Myneni *et al*., 1997), averaged over the same decade (1982–1991) as the climatological forcing data; the Global Land Cover Facility tree cover dataset (DeFries *et al*., 2000a, b); and a 1 km resolution NPP dataset for 1999 derived from SPOT-VEGETATION satellite measurements using the C-Fix methodology (http://www.geosuccess.net). LAI, NPP and tree cover data were extracted using the ISLSCP categorization for conifer forests only, and classified as either evergreen or deciduous. Modelled LAI and NPP values were weighted by the fractional cover of each LL.

Across all sites ($n = 237$) modelled LAI data exceeded the satellite data by an average of 1.6 ($m^2\,m^{-2}$), with a standard deviation of the differences of 1.9. The agreement is reasonable given the test is imperfect because of the introduction of errors by methodological procedures for processing satellite data (Beerling & Woodward, 2001). Fractional tree cover also introduced another source of error. Satellites measure the LAI for a grid cell that may contain a mixture of vegetation some of which has a lower LAI than forest (e.g. grassland or tundra) or bare ground. Correcting for this effect using tree cover fraction, assuming an typical LAI for grasslands/tundra of 2.0, gives a mean error between observed and modelled of 0.18 with a standard deviation of 0.74; both datasets were significantly correlated ($r^2 = 0.34$, $P < 0.001$). A Kolmogorov–Smirnov test the 5% significance level showed that the frequency histogram of LAI errors was normally distributed. Overall, this analysis indicates there was no systematic bias in simulated forest LAIs at the regional scale.

Across all sites ($n = 237$) modelled and satellite NPP differed by an average of $-0.3\,g\,C\,m^{-2}\,yr^{-1}$ and a standard deviation of $158.2\,g\,C\,m^{-2}\,yr^{-1}$. This is a reasonable match given the large difference between the methods used to estimate NPP. Both datasets were significantly correlated ($r^2 = 0.30$, $P < 0.001$). A Kolmogorov–Smirnov test at the 5% significance level showed the frequency histogram of differences between observed and simulated lacked systematic bias and were normally distributed.

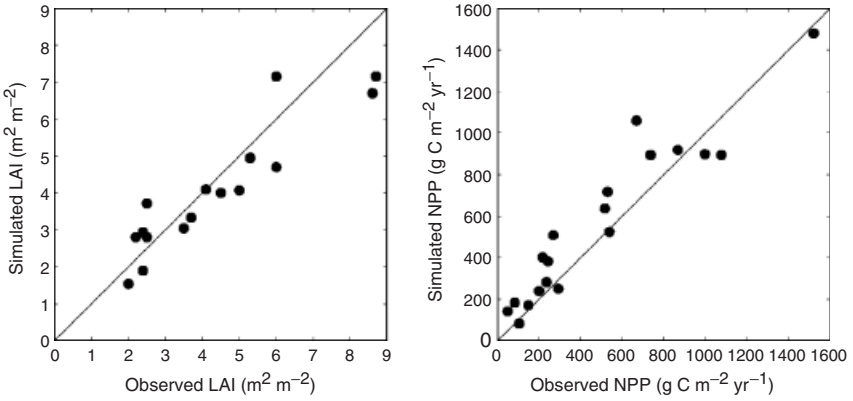

Fig. A1 Correlations between observed and measured leaf area indices (a) and net primary production of contemporary conifer forests across a wide climatic gradient. Regression details for (a) $r^2 = 0.84$, $P < 0.01$; and for (b) $r^2 = 0.89$, $P < 0.01$. See Osborne & Beerling (2002a) for dominant LLs and climatic details of sites.